Millennial- to centennial-scale changes in sea surface temperature in the tropical South Atlantic throughout the Holocene

Thiago P. Santos [a], Daniel R. Franco [b], Catia F. Barbosa [a], Andre L. Belem [a], Trond Dokken [c], Ana Luiza S. Albuquerque [a,*]

[a] Departamento de Geoquímica, Universidade Federal Fluminense, Outeiro de São João Batista, s/nº., Niterói, Rio de Janeiro 24020-141, Brazil
[b] Coordenação de Geofísica, Observatório Nacional, Rua General José Cristino 77, Rio de Janeiro 20921-400, Brazil
[c] Bjerknes Centre for Climate Research, Allégaten 55, NO-5007 Bergen, Norway

ABSTRACT

We performed $\delta^{18}O_C$ (*Globigerinoides ruber*, 250–300 μm white) and SST (modern analogue technique) paleoceanographic reconstructions for the western tropical South Atlantic Ocean at the northeast Brazilian margin to assess millennial- to centennial-scale climatic shifts that may be propagated by the thermohaline circulation. The results show a progressive SST increase (~1 °C) over the Holocene, with a prominent shift occurring during the mid-Holocene that may be linked to changes in insolation distribution. Furthermore, spectral and coherency analyses reveal several centennial- to millennial-scale modes of variability that are similar in both proxy records (4.1–3.8 kyr, 1.5–1.0 kyr, ~700 yr, 570–560 yr, ~390 yr, ~350 yr and ~330 yr). Such variability could be the result of (1) solar-induced atmospheric changes at northern high latitudes (possibly propagated southward by the meridional overturning circulation and hence inducing shifts in tropical $\delta^{18}O_c$ and sea surface temperature), and/or (2) salinity anomalies propagated from the Southern Atlantic Ocean and transmitted to the study site through the Agulhas Leakage. These climate oscillations may have had substantive effects on the Holocene climate system, especially over the tropical western South Atlantic Ocean and the South American continent. Our data show that the western tropical South Atlantic may respond to multi-centennial to millennial oscillations that are possibly triggered by external (solar) and internal (northern and southern high latitudes) climate forcing. Further investigations are necessary to illuminate the role of the western tropical South Atlantic in interhemispheric heat transfer.

© 2013 Elsevier B.V. All rights reserved.

1. Introduction

Recently developed paleoclimate records of the Holocene show that the warm climate of the most recent 11,000 calendar years before present (cal yr BP) was unstable and punctuated by several significant millennial- and centennial-scale climate variations (Alley et al., 1997; Bond et al., 1997; McDermott et al., 1999, 2001; Mayewski et al., 2004; Darby et al., 2012; Olsen et al., 2012). Abrupt changes in the Atlantic meridional overturning circulation (AMOC) have been speculated to be an important mechanism in spreading these periodic events worldwide via changes in meridional heat transport (Menary et al., 2011).

These periodicities were first described for the Northern Atlantic (Bond et al., 1997; Bianchi and McCave et al., 1999) as a sequence of inputs of large amounts of fresh water from the retreat of the Laurentide ice sheet, which disrupted the thermohaline circulation and triggered rapid sea surface temperature (SST) cooling in the region. The recurrence of such temperature variability is typically associated with both

insolation changes and the ocean–atmosphere coupling that played a prominent role in the dynamics of the Holocene climate (Morley et al., 2011).

Because high-latitude and low-latitudes climates are interconnected by ocean–atmosphere coupling, the influence of cooling events in the North Atlantic extends beyond the immediate region and has profound implications for the restructuring of tropical climate patterns (deMenocal et al., 2000). These climate changes involve pervasive droughts, glacier expansions and precipitation increases that have affected several human populations in the last thousand years (Hodell et al., 2001; Wanner et al., 2008). Recent general circulation modeling studies (e.g., Sutton et al., 2000) indicate that most of the tropical Atlantic SST variability is due to an equatorward extension of various extra-tropical patterns, especially the North Atlantic Oscillation (NAO). Teleconnections between the NAO and southern regions, notably the Agulhas Leakage, cannot be ruled out (Gasse et al., 2008).

Due to its importance in exporting heat northward through meridional overturning, the western tropical Atlantic region is critical to the development of the long-term climate system. In this paper, we focus on the evolution of millennial- to centennial-scale cycles of SST in the tropical South Atlantic during the Holocene using oxygen stable isotopes from

* Corresponding author. Tel.: +55 21 2629 2197.
  E-mail address: ana_albuquerque@id.uff.br (A.L.S. Albuquerque).

planktonic foraminifera ($\delta^{18}O_c$) and the Modern Analogue Technique (MAT).

2. Materials and methods

2.1. Study area

The cores GS07-150 17/2 (04º12.986S, 37º04.518 W) and GS07-150 11/1 (04º45.314S, 35º03.351 W), hereafter abbreviated as MC 17/2 and MC 11/1, were collected in 2007 during the R/V *G.O. Sars* cruise in the western tropical Atlantic at depths of 1000 m and 730 m on the upper continental slope, respectively (Fig. 1). The sample sites are located in the Potiguar sedimentary basin and are separated by only 230 km.

The study area falls under the influence of the North Brazil Current (NBC), the primary northward export channel of heat and salt from the South Atlantic Ocean. The NBC originates from a split where the South Equatorial Current (SEC) reaches the South American continent, which causes it to branch northward. The NBC is a weak surface flow associated with a strong deep component, the North Brazil Under Current (NBUC) (Stramma et al., 1995; Boebel et al., 1999), which exhibits seasonal behavior. Thus, between July and February, the surface layer of the NBC separates from the coast and retroflects, contributing to the flow of the North Equatorial Countercurrent (NECC). From March through June, most of the NBC continues northwestward along the South American coast and continental slope (Fonseca et al., 2004).

These upper-level currents are controlled by seasonal variations in the position of the Intertropical Convergence Zone (ITCZ) (Wilson et al., 2011), which influences the heat flux and, through evaporation and precipitation of water mass in the area. The continental area of northeast Brazil contributes minimal water mass to the offshore region due to its semi-arid climate and the presence of only small rivers whose discharges do not greatly influence the adjacent ocean (Arz et al., 1999).

2.2. Age-depth modeling

The cores MC 17/2 (20 cm in length) and 11/1 (15 cm in length) were sliced every 0.5 cm. Due to their abundance, the planktonic foraminifera *Globigerinoides ruber* (white) were sorted over a 150-μm mesh to be dated by AMS ^{14}C radiocarbon at the NSF-Arizona AMS facility, which used 0.005 g of each sample. A total of eight AMS ^{14}C radiocarbon dates were measured (Table 1).

Age-depth modeling was conducted using Clam 2.1 (Blaauw, 2010) software, applying Bayesian statistics. A small overlapping of ages was identified in the last centimeter of the core MC 17/2; because of this, this portion of the core was eliminated from the analysis. ^{14}C ages were calibrated using the curve Marine09 (Reimer et al., 2009) with a standard marine correction of 400 years and were linearly interpolated at 95% confidence ranges (Fig. 2). The top of core MC 17/2 was dated at 670 calendar years before present (cal yr BP) and the bottom at 3725 cal yr BP. The top of core MC 11/1 was dated at 3825 cal yr BP and the bottom at 11820 cal yr BP.

To provide a single age model covering the Holocene, data for each type of proxy from cores MC 17/2 and 11/1 were merged into two single $\delta^{18}O$ and SST_{MAT} data series (Fig. 4). Such an approach has been successfully used in reconstructions based on marine records (Budziak et al., 2000; Nielsen et al., 2004; Singh et al., 2011), lacustrine sediments (Enters et al., 2006; Mayr et al., 2007) and speleothems (Strikis et al., 2011). The two resulting $\delta^{18}O$ and SST_{MAT} data series (with n = 73) covered the time interval of 12030–673 cal yr BP (timespan of ~11.3 kyr) and exhibited sample rate intervals of 56–368 yr (Fig. 4D).

The overlapping between the cores includes only two samples but was not a significant problem because the $\delta^{18}O$ data were continuous across the transition, and the primary change in the individual planktonic foraminifera species occurred slightly earlier than the core break. This is discussed in the following sections.

2.3. Planktonic foraminifera assemblage and MAT

A 1-cm^3 sample of planktonic foraminifera fauna sediment from both cores was analyzed after being washed over a 150-μm mesh sieve and oven-dried. We first split the samples until a minimum of 300 shells remained. They were identified, based on data collected from previous studies (Parker, 1962; Bé, 1977; Kennett and Srinavasam, 1983), using stereomicroscopy. The quantity of each species is presented as the relative abundance.
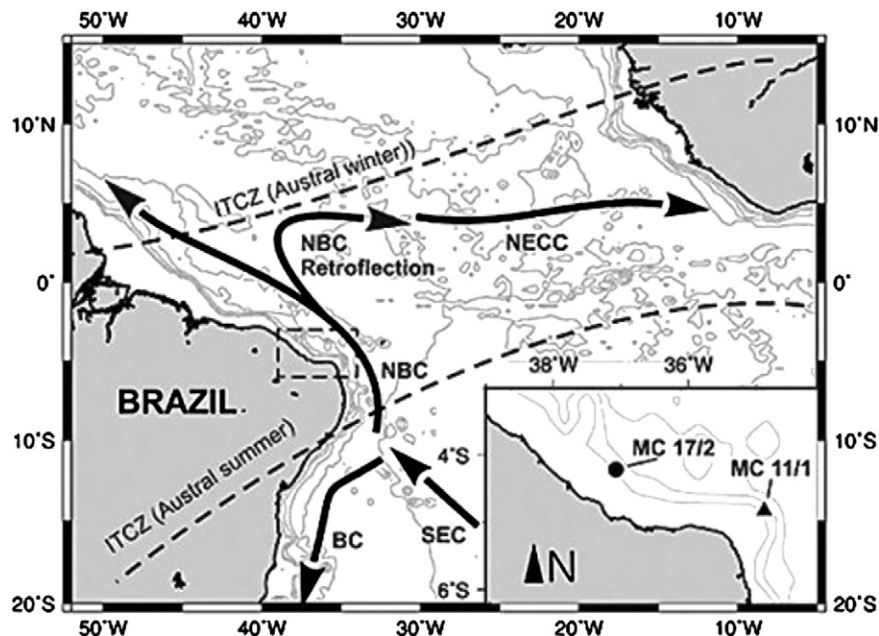

Fig. 1. Map showing the study area with a schematic illustration of the mean surface circulation off of the Northeast Brazilian Margin. The currents are: SEC — South Equatorial Current, BC — Brazil Current, NBC — North Brazil Current and its retroflection, NECC — North Equatorial Countercurrent. The dashed lines represent the seasonal position of the ITCZ — Intertropical Convergence Zone.

Table 1
AMS radiocarbon ages of the selected samples. Calibrated ages were linearly interpolated using a Bayesian statistical model with Clam 2.1 software (Blaauw, 2010) and the Marine09 curve (Reimer et al., 2009).

Lab Code	Core	Sample (cm)	Age ^{14}C BP	Age ^{14}C error	cal year BP	Min. age (cal yr BP)	Max. age (cal yr BP)
AA89721	MC 17/2	2	1528	47	1070	943	1243
AA89722	MC 17/2	5.5	2166	47	1765	1583	1914
AA89723	MC 17/2	10	2644	47	2269	2115	2463
AA89724	MC 17/2	19.5	4369	50	4510	4334	4759
AA90167	MC 11/1	2	4958	39	5295	5122	5440
AA90168	MC 11/1	5	7008	70	7500	7304	7678
AA90169	MC 11/1	10	8922	79	9450	9340	9977
AA90170	MC 11/1	15	10,449	91	11,615	11,208	12,076

To assess the SST, MAT was conducted using the software PAST and a South Atlantic database composed of a compilation of CLIMAP and MARGO top-core datasets (n = 468). Each sample of both cores was compared with the five best analogs in the modern database to reconstruct the SST. The Square Chord function was used as the distance measure, and the relationship between the observed SST and the reconstructed SST showed a correlation of $R^2 = 0.9807$ (P > 95%).

2.4. Oxygen stable isotope

The $\delta^{18}O_c$ analyses from the tests were based on 15 specimens of *Globigerinoides ruber* (white) from a 250–300 μm fraction. The analyses were performed at the Stable Isotope Laboratory at the University of California using a Finning MAT 252 spectrometer with a precision of ±0.04‰. The samples were reacted in 105% H_3PO_4 at 90 °C using a Gilson Multicarb Autosampler. The data were adjusted to VPDB using the NBS-19 calcite standard.

2.5. Spectral analysis

To characterize the harmonic behavior of the $\delta^{18}O_c$ and the SST_{MAT} time series, we performed a spectral analysis for unevenly spaced time series using REDFIT software (Schulz and Mudelsee, 2002). The resulting spectral peaks were tested at 80, 90, 95 and 99% confidence levels based on a first-order autoregressive model fitted to the data. Coherency spectra were also calculated using the SPECTRUM software (Schulz and Stattegger, 1997) to identify possible harmonic patterns that were common to both datasets.

3. Results

3.1. Planktonic foraminifera assemblage and SST reconstruction

A total of 21 species of planktonic foraminifera were identified in the two cores. Among all observed species, nine were dominant and were considered important for the purpose of paleoceanographic interpretation (Fig. 3A). The most significant shift in planktonic foraminifera abundance was in the transition from the mid- to late-Holocene. The most abundant species were those related to warm surface waters, i.e., *Globigerinoides ruber* (50–75%) (pink and white), *Globigerinoides sacculifer* (5–25%) (with and without sac) and *Globigerinella siphonifera* (2–8%). *G. sacculifer* were inversely correlated with *G. ruber* and *G. siphonifera* (Fig. 3A).

The quantities of *Globigerinella calida* and *Globigerina glutinata* ranged between 0–2% and 2–7%, respectively, but showed no clear trend over time (Fig. 3A). Species described as thermocline dwellers, i.e., *Globorotalia menardii* (1–10%), *Pulleniatina obliquiloculata* (0–4%) and *Neogloboquadrina dutertrei* (0–4%), showed an increase in quantity over time (Fig. 3A). There was an extreme reduction in a unique deep-dweller species with significant abundance, *Globorotalia truncatulinoides* (left and right coiling) (0–2.5%): from the mid- to late-Holocene, its population nearly disappeared (Fig. 3A).

The SST_{MAT} showed an average Holocene water temperature of 27.1 °C (Fig. 3B). The temperatures were colder during the early- and mid-Holocene and rose abruptly by approximately 1 °C between the mid- and late-Holocene. During the early- and mid-Holocene, the SST showed larger amplitude variability than it did in the late-Holocene (Fig. 3B).

3.2. Oxygen isotope composition of planktonic foraminifera shells ($\delta^{18}O_c$)

Together, the two cores represent conditions over a 12-kyr range during the Holocene Epoch. MC 11/1 provides a record from the early-Holocene (11.5–8 cal kyr BP) to the mid-Holocene (8–4 cal kyr BP), and MC 17/2 provides a record of the late-Holocene (4–0.7 cal kyr BP).

The isotopic analysis of planktonic foraminifera *Globigerinoides ruber* white (250–300 μm) was split into three intervals (early-, mid- and late-Holocene). The isotopic values decreased monotonically over time (Fig. 4C). The data showed a range of 1.08‰ over the Holocene, with the highest and lowest values occurring at approximately 8 cal kyr BP and 1.5 cal kyr BP, respectively. The average $\delta^{18}O_c$ value was −1.2‰ for the early-Holocene, −1.52‰ for the mid-Holocene and −1.81‰ for the late-Holocene, with a mean reduction of −0.61‰ over time (Fig. 4C).
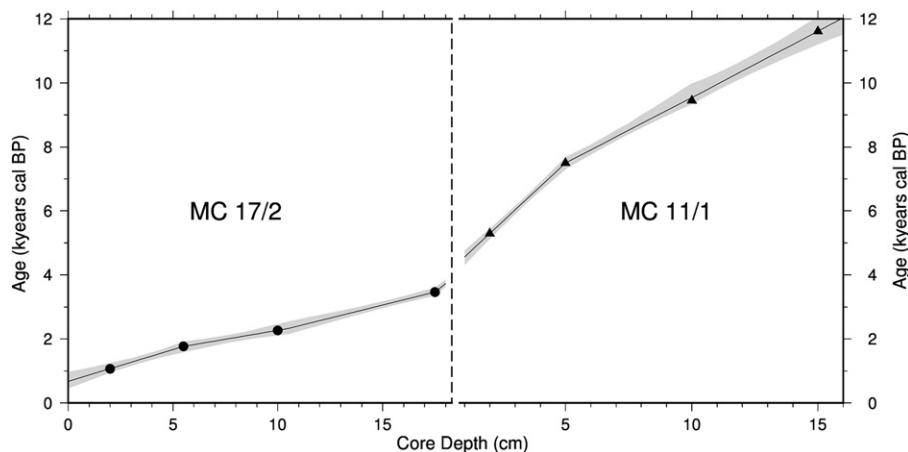

Fig. 2. Age-depth modeling was constructed with the software Clam 2.1 (Blaauw, 2010), applying a Bayesian statistical method. The chronologies of the two cores were combined to generate an age model that is unique to the Holocene. The ^{14}C ages were linearly interpolated through the Marine09 curve (Reimer et al., 2009).
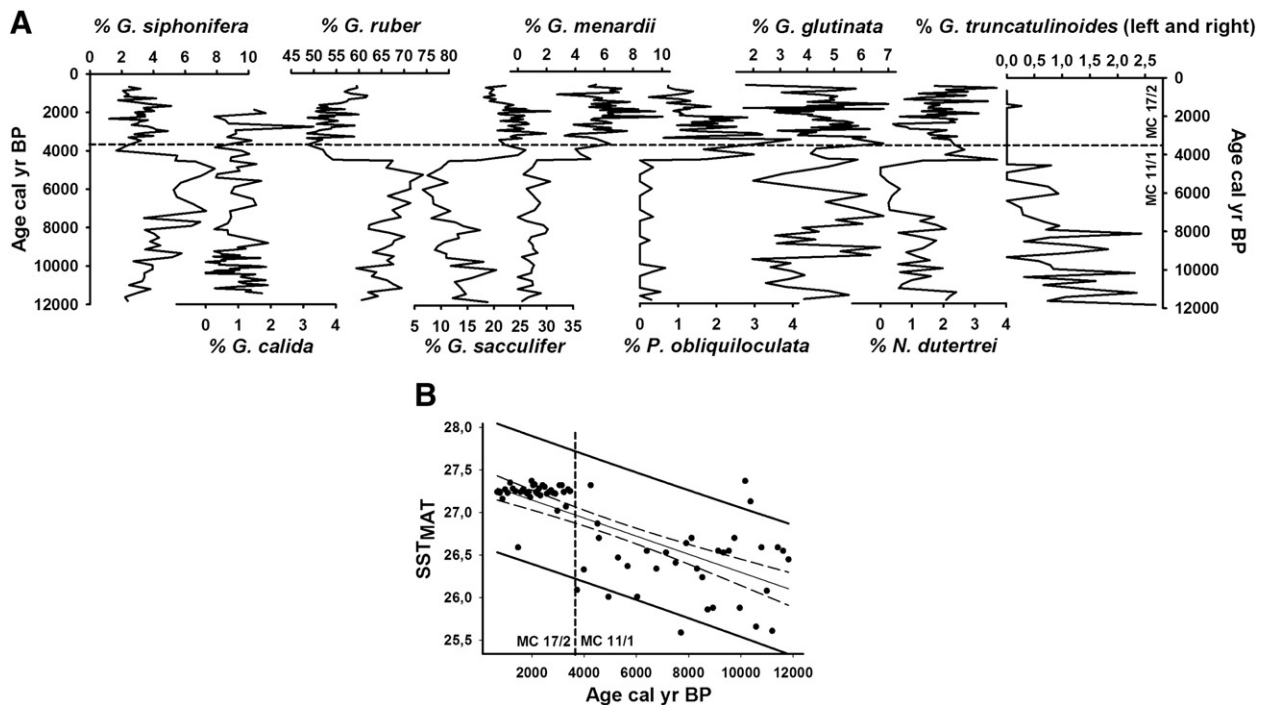
Fig. 3. A: Relative abundances of the main species of planktonic foraminifera from the cores MC 11/1 and MC 17/2. B: linear regression of the reconstructed temperatures. Solid line is the 95% confidence band and the dashed line is the 95% prediction band.

4. Discussion

4.1. Spectral analysis: millennial to centennial oscillatory modes

Spectral analysis of the $\delta^{18}O_c$ and SST_{MAT} datasets (Fig. 5) revealed a wide range of multi-centennial to millennial harmonic features. These seem to be coherent for both proxies at an 80% confidence level (Fig. 6). To assess the possible factors causing these oscillations, the observed harmonic features were grouped in distinctive ranges of oscillatory modes: (i) 4.1–3.8 kyr, (ii) 1.5–1.0 kyr (millennial timescale), (iii) ~700 yr, (iv) 570–560 yr and (v) 390–330 yr (centennial timescale).

4.2. Millennial-scale harmonic features

The millennial component of the time series is evidenced by two ranges, or 'bands', of oscillatory modes: (i) 1.5–1.0 kyr (spectral peaks at 1498 yr (Fig. 5A), 1212 yr and 1001 yr (Fig. 5B)) and (ii) 4.1–3.8 kyr (spectral peaks at 4085 yr, 1498 yr (Fig. 5A) and 3838 yr (Fig. 5B)). A prominent spectral peak at ~12 kyr (Fig. 5B) is proportional to the entire length of the SST_{MAT} dataset and thus was not considered in our results.

Sub-Milankovitch harmonic features observed in the spectral band at 4.1–3.8 kyr are compatible with the millennial-scale climatic variability reported in Quaternary paleoarchives by several authors (e.g., Pokras and Mix, 1987; Bond et al., 1993; Keigwin and Jones, 1994; Bard, 2002; Wanner et al., 2008; Franco et al., 2012). Chapman and Shackleton (1998, 1999) reported that such high-frequency variability may be a non-linear response of the climate system to tones from the combination of the precession and obliquity harmonics. The presence of such strong precession-related signals suggests that cross-equatorial heat transport, which may involve NBC activity, is a major factor controlling the surface oceanography of the mid-latitude North Atlantic (Chapman and Shackleton, 1998).

The spectral band from 1.5 to 1.0 kyr in particular is quite compatible with the so-called Bond events, sequences of ice-rafting episodes that were identified in North Atlantic records at a pacing of ~1500 years
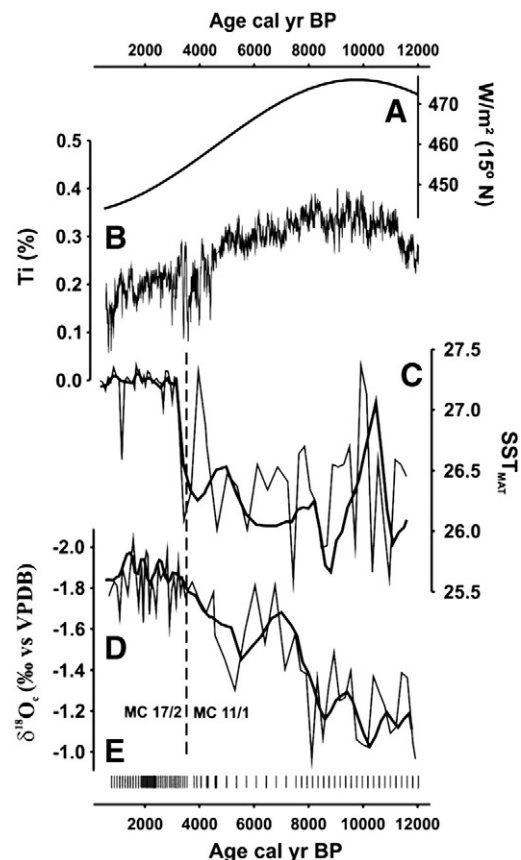

Fig. 4. A: Extraterrestrial insolation (W/m²) at 15° N for the Holocene (Niedermeyer et al., 2010). B: Ti (%) of the Hole 1002C from the Cariaco Basin (Haug et al., 2001). C: composite SST reconstructed by MAT (SST_{MAT}) for the cores MC 11/1 and 17/2. D: composite *G. ruber* (white 250–300 μm) $\delta^{18}O_c$ record from the cores MC 11/1 and 17/2. D: distribution of sampling intervals for $\delta^{18}O_c$ and SST_{MAT} datasets (ranging from 50 to 368 years). Solid lines are associated with smoothed curves (10% weighted average) for the SST_{MAT} and $\delta^{18}O_c$ datasets (thin lines).
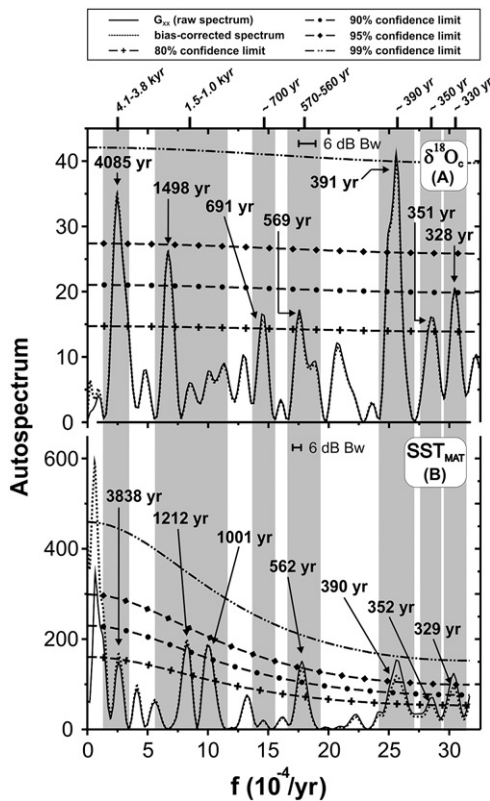
Fig. 5. Harmonic content in the $\delta^{18}O_c$ (A) and SST_{MAT} (B) datasets as revealed by REDFIT software for unevenly spaced time series (Schulz and Mudelsee, 2002). Resulting spectral peak contents were associated with significance tests at 80, 90, 95 and 99% confidence limits based on a first-order autoregressive model fitted to the data.

(Bond et al., 1993, 1997; Dima and Lohmann, 2009; Strikis et al., 2011). Most discussions of this millennial-scale oscillation focus on Northern Hemisphere records and oceanic circulation models; however, there have been increasing reports of a globally coherent, millennial-scale pattern of climate variability that is compatible with these variations recorded by continental and marine palaeoarchives (e.g., Bianchi and McCave, 1999; Chapman and Shackleton, 1999; Hinnov et al., 2002; Debret et al., 2009). Recently, the 1500-yr pacing has been discussed for different paleoclimatic archives from the Southern Hemisphere, including Antarctic paleotemperature datasets (Blunier and Brook, 2001), diatom assemblages from South Atlantic marine sedimentary sequences (Nielsen et al., 2004), the Holocene marine record from the tropical western Atlantic (Arz et al., 2001) and continental ice cores and
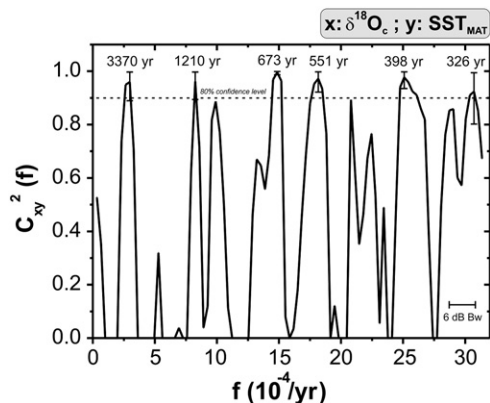

Fig. 6. Coherency spectra found using the SPECTRUM software (Schulz and Stattegger, 1997), showing that some harmonic patterns are commonly observed in both datasets.

lacustrine sequence datasets from South America (e.g., Thompson, 2000; Lamy et al., 2001).

Although the nature of its pacing, driving mechanism and the mechanism of interhemispheric propagation through the atmosphere–ocean system are still under debate (Pena et al., 2010), such a millennial-scale pattern characterizes the most prominent Holocene climate oscillations. Its occurrence has been linked to large-scale spatial variations in oceanic thermohaline circulation due to changes in the formation of North Atlantic Deep Water (NADW) (Hoogakker et al., 2011; Darby et al., 2012). Variability in NADW formation may produce changes in the Atlantic Meridional Overturning Circulation (AMOC) pattern similar to those observed during Heinrich Event 1, in which a near-total shutdown of the AMOC was observed (McManus et al., 2004). Although ice-rafting events in the Holocene have occurred less frequently than during the last glacial period (Moros et al., 2004), possible fluctuations in the interhemispheric heat transfer due to the AMOC activity, which may follow a ~1500-yr pacing, cannot be ruled out as a driving factor for environmental changes.

As evidence for a southward, interhemispheric propagating mechanism for the 1500-yr pacing, Pena et al. (2010) argued that the primary source of this periodicity could be located somewhere at high latitudes in the Northern Hemisphere and that the climatic signal would be rapidly propagated southward. They suggested that such phenomena could be explained by means of southward shifts in the atmospheric–oceanic coupled system, which would extend the solar impact on the climate from polar to tropical latitudes, which would alter hemispheric SST gradients and, potentially, the climate response in lower-latitude regions. A possible consequence of this climatic pacing is the successive short-term excursions of ~0.3–0.5‰ and ~0.5 °C in the $\delta^{18}O_c$ and SST_{MAT} datasets, respectively. Such a millennial-scale warming trend may be linked with weak NBC inter-hemispheric heat transfer due to a reduction in the NADW formation rate, which could contribute to increased moisture advection into South America, as the continental reconstruction also reported a linkage with the 1500-year pacing (Baker et al., 2005; Strikis et al., 2011).

4.3. Centennial-scale harmonic features

Holocene centennial-scale oscillations evidenced in inter-hemispheric paleoclimatic archives have been extensively reported, but the underlying mechanisms causing them are still not well understood (e.g., Risebrobakken et al., 2003; Baker et al., 2005; Rousse et al., 2006; Delworth and Zeng, 2012), which prevents a straightforward interpretation of the centennial-scale bands observed in this study. Nevertheless, we note here some particularities for these multi-centennial bands.

The centennial bands centered at ~700 yr and 570–560 yr (Fig. 5A and B) are quite similar to the 550–500-yr periodicity reported by various studies and suggest a ~650–400-yr pervasive mode throughout the Holocene (e.g., Hall et al., 2004; Rohling and Pälike, 2005). For instance, similar centennial-scale oscillations were reported by Chapman and Shackleton (1998) from sedimentological color datasets measured in sediment from a North Atlantic deep-sea core that was believed to be under the influence of the Iceland-Scotland Overflow Water. The authors related this periodicity to deep-ocean circulation changes, which may affect the western tropical Atlantic in a similar way as it does the 1500-year cycle. Arz et al. (2001) ascribed a 510-year harmonic feature to the western tropical Atlantic and found other centennial- to millennial-scale oscillations centered at 1540 and 730 years. These authors argued that such variability might be an expression of internally forced oscillations of the ocean–atmosphere system. For instance, the observed equatorward displacement of the westerlies associated with an expanded polar vortex over Greenland could have resulted in an episodically enhanced trade-wind circulation at tropical latitudes, which may have affected the intensity of the NBC and therefore contributed to changes in the influx of heat and salt into the North Atlantic. The

centennial bands on Fig. 5A and B suggest that a mechanism amplifying Holocene climate variation in tropical latitudes may be linked to deep-water-generating processes at high latitudes.

The most recent centennial-scale bands, centered at ~390 yr, ~350 yr and ~330 yr, could be consequences of the same process that strongly influences the sedimentation process at the study area, as is suggested by the prominent 391-yr spectral peak in the $\delta^{18}O_c$ spectrum (Fig. 5A) and other low-power spectral peaks (Fig. 5A and B). Notably, a ~390–330 yr periodic signature has been reported by several studies of various worldwide Holocene palaeoarchives (e.g., Bond et al., 2001; Poore, 2003; Hall et al., 2004; Skillbeck et al., 2005). For instance, in a lacustrine $\delta^{13}C$ record from South America, Baker et al. (2005) identified multiple multi-centennial oscillatory modes that may be linked to centennial-scale solar variability. They indicate an out-of-phase relationship between the precipitation variability on the Altiplano in Bolivia and Peru and the Northern Hemisphere monsoonal precipitation over the Holocene. Similarly, Ekdahl et al. (2008) reported a centennial-scale periodic range for diatom assemblage datasets obtained from lacustrine sedimentary cores from the Altiplano that could be linked to the ~350-yr variability they found in the ^{10}Be production rate.

High-resolution magnetic analyses off of North Iceland indicated that possible effects of the NAO could be associated with centennial-scale variability (Rousse et al., 2006). The NAO index likely exhibited more positive values during the mid-Holocene and more negative values during the late-Holocene (Wanner et al., 2008). This behavior may be strongly influenced by the observed variability in the westerly wind stress, which could lead to a freshening of the northern North Atlantic and to a consequent weakening of the heat transfer from the tropics, which would reorganize coupled oceanic–atmospheric patterns. A 4000-yr model simulation of surface air temperature recently run by Delworth and Zeng (2012) suggested that the meridional propagation of Southern Ocean fresh water anomalies may suppress convective processes and weaken the AMOC, consequently reducing salinity in the North Atlantic at high latitudes and setting the pace for multi-centennial AMOC variations. The Agulhas Leakage could be the pathway through which such salinity anomalies would reach the western tropical South Atlantic (Gasse et al., 2008). Accordingly, factors, such as the change in the NAO index from generally positive to generally negative during the mid- to late-Holocene and the propagation of fresh water signals through the entire latitudinal extent of the Atlantic, may control the AMOC intensity and the shift in the tropical $\delta^{18}O_c$ and SST_{MAT} signal.

4.4. Variability in the western tropical South Atlantic during the Holocene

The terrigenous input into the Atlantic from the northeastern Brazilian continental slope decreased significantly from its Last Glacial Maximum (LGM) value after Heinrich event 1 and the Younger Dryas (Jaeschke et al., 2007). This indicates that the gradual decrease of $\delta^{18}O_c$ during the Holocene was not caused by the intrusion of isotopically lighter water from the continent. Without taking into account the ice-volume component, which is negligible during the most recent 5 kyr of the Holocene (Guilderson and Pak, 2007), our $\delta^{18}O_c$ signal responds to variability in temperature, evaporation and salinity, exhibiting similar trends as the SST reconstruction by MAT. Assuming the formula 0.22‰ per °C, a mean reduction of 0.61‰ in $\delta^{18}O_c$ would generate a SST increase of almost 3 °C (Rühlemann et al., 2004), which is implausible for the Holocene. The SST_{MAT} reconstruction shows that the temperature rise over the Holocene was slightly greater than 1 °C (Fig. 4B). We can assume that the difference between the two proxies is due to the influence of evaporation and salinity variability on the $\delta^{18}O$ of the seawater. The increase in SST calculated by the MAT from the mid- to late-Holocene was most likely influenced by the species G. sacculifer, G. menardii and P. obliquiloculata, which doubled in abundance over this time period, as well as by the near disappearance of G. truncatulinoides (left and right

coiling) (Fig. 3A), which provides ecological evidence of the observed climate change.

The general warming trend over the Holocene in the tropical Atlantic was accompanied by cooling in the eastern North Atlantic and the Mediterranean Sea (Marchal et al., 2002) and on the Greenland ice sheet (Vinther et al., 2009). Data from model simulations (Mayewski et al., 2004; Lorenz et al., 2006) showed that changes in precession and obliquity cycles caused a variation in the solar energy distribution; the most pronounced radiative change was a decrease in boreal summer insolation in the northern latitudes accompanied by an increase in boreal winter insolation in the southern latitudes. This change may explain the shift in $\delta^{18}O_c$ and SST_{MAT}, primarily in the mid- to late-Holocene (Fig. 4). In this interval, the climate system underwent a wide reorganization due to changes in orbital forcing and the redistribution of solar energy on a millennial timescale (Wanner et al., 2008; Wirtz et al., 2010).

The reduction in summer insolation in northern regions warmed the southern tropics, accentuating the temperature gradient between the hemispheres and causing a summer southward displacement of the ITCZ. This displacement, recorded in proxy data (Haug et al., 2001; Wang et al., 2005; Yu et al., 2006; Bernal et al., 2011), brought cold, dry conditions over northern tropical locations in several parts in the world, such as southwestern Mexico, southern and northwest China and in the Cariaco Basin. However, the southward displacement of the ITCZ induced wetter conditions over the South American continent, especially in the regions under the influence of the South American monsoon system (SAMS). Dahl et al. (2005) and Broccoli et al. (2006) demonstrated through an ocean/atmosphere circulation model that freshening of the water at northern high latitudes not only induces SST anomalies and ITCZ displacement but also increases moisture advection from the tropical Atlantic onto the South American continent by strengthening the northeast trade winds.

Such moisture advection during North Atlantic freshening events may intensify precipitation patterns over the South American continent, as shown by Baker et al. (2005) and Ekdahl et al. (2008) at the South American Altiplano or even further south through modulation of the tropical climate system through Hadley cell intensity (Lamy et al., 2001). Poore (2003) reported a decrease in G. sacculifer abundance in the Gulf of Mexico from 6 cal kyr BP and attributed it to a southerly position of the ITCZ, which reduced the transport of Caribbean surface waters into the region. However, our G. sacculifer data show higher abundances at 6 cal kyr BP (Fig. 3A) than at earlier periods in the core, indicating that the southward movement of the ITCZ during the Holocene favored the transport of warm and saline waters to the western tropical Atlantic, primarily after the mid-Holocene.

5. Summary

By studying a combination of two sediment multicores, namely the $\delta^{18}O_c$ of planktonic foraminifera Globigerinoides ruber (250–300 μm white) and SST_{MAT}, that were recovered from the western tropical South Atlantic Ocean on the northeast Brazilian margin, we reconstructed the SST record over the Holocene. These two proxies showed a progressive warming trend of slightly more than 1 °C. The main shift in SST occurred during the transition from the mid- to late-Holocene, when changes in orbital parameters and insolation distribution played an important role in warming the Southern Hemisphere. The temperature gradient that developed in the Atlantic Ocean displaced the ITCZ farther south and affected the SEC, transporting more warm waters to the western tropical South Atlantic, as has been noted by several continental-based climate reconstructions.

The spectral analyses conducted on the two proxies showed a series of millennial- to centennial-scale cycles at frequencies of 4.1–3.8 kyr, 1.5–1.0 kyr, ~700 yr, 570–560 yr, ~390 yr, ~350 yr and ~330 yr. The coherency spectra between $\delta^{18}O_c$ and SST_{MAT} reinforced the persistence of climate variability, with peaks centered at 3370 yr, 1210 yr, 673 yr,

551 yr, 398 yr and 326 yr. Variability at these periods has been found in several paleoclimatological records around the world, mainly in the 1.5–1.0-kyr cycle. The presence of this mode of variability in our data may be a reflection of solar-induced atmospheric changes that spread globally through their impact in northern high latitudes, which affected the AMOC intensity and shifted tropical $\delta^{18}O_c$ and SST_{MAT} trends. These cyclical events disrupted the North Atlantic thermohaline circulation and reduced the northward heat transport from the tropical Atlantic. Coupled with the possible influence of the northern Atlantic, centennial-scale salinity anomalies released from the Southern Ocean may have reached the western tropical South Atlantic and affected the AMOC, bringing profound consequences to the Holocene climate system, especially over South America, where the moisture balance was altered due to the southward shift of the ITCZ and the intensification of SAMS.

Acknowledgements

Appendix A. Supplementary data

Supplementary data associated with this article can be found in the online version, at http://dx.doi.org/10.1016/j.palaeo.2013.08.019. These data include Google map of the most important areas described in this article.

References

Alley, R.B., Mayewski, P.A., Sowers, T., Stuiver, M., Taylor, K.C., Clark, P.U., 1997. Holocene climatic instability: a prominent widespread event 8200 years ago. Geology 25, 483–486.

Arz, H., Patzold, J., Wefer, G., 1999. The deglacial history of the western tropical Atlantic as inferred from high resolution stable isotope records off northeastern Brazil. Earth and Planetary Science Letters 167 (1–2), 105–117.

Arz, H., Gerhardt, S., Patzold, J., Rohl, U., 2001. Millennial-scale changes of the surface and deep-water flow in the western tropical Atlantic linked to Northern Hemisphere high-latitude climate during the Holocene. Geology 29 (3), 239–242. http://dx.doi.org/10.1130/0091-7613.

Baker, P.A., Fritz, S.C., Garland, J., Ekdahl, E., 2005. Holocene hydrologic variation at Lake Titicaca, Bolivia/Peru, and its relationship to North Atlantic climate variation. J. Quat. Sci. 20 (7–8), 655–662. http://dx.doi.org/10.1002/jqs.987.

Bard, E., 2002. Climate Schock: Abrupt changes over millennial time scales. Physics Today 55, 32–37.

Bé, A.W.H., 1977. An ecological, zoogeographic and taxonomic review of recentplanktonic foraminifera. In: Ramsay, A.T.S. (Ed.), Oceanic Micropaleontology. Academic Press, London, pp. 1–100.

Bernal, J.P., Lachniet, M., McCulloch, M., Mortimer, G., Morales, P., Cienfuegos, E., 2011. A speleothem record of Holocene climate variability from southwestern Mexico. Quat. Res. 75 (1), 104–113. http://dx.doi.org/10.1016/j.yqres.2010.09.002.

Bianchi, G.G., McCave, N., 1999. Holocene periodicity in North Atlantic climate and deep-ocean flow south of Iceland. Nature 397, 515–517. http://dx.doi.org/10.1038/17362.

Blaauw, M., 2010. Methods and code for 'classical' age-modelling of radiocarbon sequences. Quat. Geochronol. 5, 512–518.

Blunier, T., Brook, E.J., 2001. Timing of millennial-scale climate change in antarctica and greenland during the last glacial period. Science 291 (5501), 109–112. http://dx.doi.org/10.1126/science.291.5501.109.

Boebel, O., Davis, R.E., Ollitrault, M., Peterson, R.G., Richardson, P.L., Schmid, C., Zenk, W., 1999. The intermediate depth circulation of the western South Atlantic. Geophys. Res. Lett. 26 (21), 3329–3332. http://dx.doi.org/10.1029/1999GL002355.

Bond, G., Broecker, W., Johnsen, S., McManus, J., Labeyrie, L., Jouzel, J., Bonani, G., 1993. Correlations between climate records from North Atlantic sediments and Greeland ice. Nature 365, 143–147.

Bond, G., Showers, W., Cheseby, M., Lotti, R., Almasi, P., deMenocal, P., Priore, P., Cullen, H., Hajdas, I., Bonani, G., 1997. A pervasive millennial-scale cycle in North Atlantic Holocene and glacial climates. Science 278 (5341), 1257–1266. http://dx.doi.org/10.1126/science.278.5341.1257.

Bond, G., Kromer, B., Beer, J., Muscheler, R., Evans, M.N., Showers, W., Hoffmann, S., Lotti-Bond, R., Hajdas, I., Bonani, G., 2001. Persistent solar influence on North Atlantic

climate during the Holocene. Science 294 (5549), 2130–2136. http://dx.doi.org/10.1126/science.1065680.

Broccoli, A.J., Dahl, K. a, Stouffer, R.J., 2006. Response of the ITCZ to Northern Hemisphere cooling. Geophys. Res. Lett. 33 (1), 1–4. http://dx.doi.org/10.1029/2005GL024546.

Budziak, D., Schneider, R.R., Rostek, F., Müller, P.J., Bard, E., Wefer, G., 2000. Late Quaternary insolation forcing on total organic carbon and C37 alkenones variations in the Arabian Sea. Paleoceanography 15 (3), 307–321.

Chapman, M.R., Shackleton, N.J., 1998. Milennial-scale fluctuation in North Atlantic heat flux during the last 150,000 years. Earth Planet. Sci. Lett. 159, 57–70.

Chapman, M.R., Shackleton, N.J., 1999. Global ice-volume fluctuation, North Atlantic ice-rafting events, and deep-ocean circulation changes between 130 and 70 ka. Geology 27, 795–798. http://dx.doi.org/10.1130/0091-7613.

Dahl, K. a, Broccoli, A.J., Stouffer, R.J., 2005. Assessing the role of North Atlantic freshwater forcing in millennial scale climate variability: a tropical Atlantic perspective. Clim. Dyn. 24 (4), 325–346. http://dx.doi.org/10.1007/s00382-004-04995.

Darby, D.A., Ortiz, J.D., Grosch, C.E., Lund, S.P., 2012. 1,500-year cycle in the Arctic Oscillation identified in Holocene Arctic sea-ice drift. Nat. Geosci. 5 (12), 897–900. http://dx.doi.org/10.1038/ngeo1629.

Debret, M., Sebag, D., Crosta, X., Massei, N., Petit, J.-R., Chapron, E., Bout-Roumazeilles, V., 2009. Evidence from wavelet analysis for a mid-Holocene transition in global climate forcing. Quat. Sci. Rev. 28, 2675–2688. http://dx.doi.org/10.1016/j.quascirev.2009.06.005.

Delworth, T.L., Zeng, F., 2012. Multicentennial variability of the Atlantic meridional overturning circulation and its climatic influence in a 4000 year simulation of the GFDL CM2. 1 climate model. Geophys. Res. Lett. 39, 1–6. http://dx.doi.org/10.1029/2012GL052107.

deMenocal, P., Ortiz, J., Guilderson, T., Sarnthein, M., 2000. Coherent high- and low-latitude climate variability during the Holocene warm period. Science 288 (5474), 2198–2202. http://dx.doi.org/10.1126/science.288.5474.2198.

Dima, M., Lohmann, G., 2009. Conceptual model for millennial climate variability: a possible combined solar-thermohaline circulation origin for the 1,500-year cycle. Clim. Dyn. 32, 301–311. http://dx.doi.org/10.1007/s00382-008-0471-x.

Ekdahl, E.J., Fritz, S.C., Baker, P. a, Rigsby, C. a, Coley, K., 2008. Holocene multidecadal- to millennial-scale hydrologic variability on the South American Altiplano. The Holocene 18 (6), 867–876. http://dx.doi.org/10.1177/0959683608093524.

Enters, D., Kirchner, G., Zolitschka, B., 2006. Establishing a chronology for lacustrine sediments using a multiple dating approach — a case study from the Frickenhauser See, central Germany. Quat. Geochronol. 1 (4), 249–260. http://dx.doi.org/10.1016/j.quageo.2007.01.005.

Fonseca, C.A., Goni, G.J., Johns, W.E., Campos, E.J.D., 2004. Investigation of the North Brazil Current retroflection and North Equatorial Countercurrent variability. Geophys. Res. Lett. 31 (21), L21304. http://dx.doi.org/10.1029/2004GL020054.

Franco, D.R., Hinnov, L.A., Ernesto, M., 2012. Millennial-scale climate cycles in Permian–Carboniferous rhythmites: permanent feature throughout geologic time? Geology. http://dx.doi.org/10.1130/G32338.1.

Gasse, F., Chalié, F., Vincens, A., Williams, M.A.J., Williamson, D., 2008. Climatic patterns in equatorial and southern Africa from 30,000 to 10,000 years ago reconstructed from terrestrial and near-shore proxy data. Quat. Sci. Rev. 27, 2316–2340.

Guilderson, T.P., Pak, D.K., 2007. Salinity Proxies $\delta^{18}O$. In: Elias, S.A. (Ed.), Encyclopedia of Quaternary, 1. Elsevier. ISBN: 978-0-444-52747-9, pp. 1766–1775.

Hall, I.R., Bianchi, G.G., Evans, J.R., 2004. Centennial to millennial scale Holocene climate-deep water linkage in the North Atlantic. Quat. Sci. Rev. 23, 1529–1536. http://dx.doi.org/10.1016/j.quascirev.2004.04.004.

Hinnov, L.A., Schulz, M., Yiou, P., 2002. Interhemispheric space-time attributes of the Dansgaard-Oeschger oscillations between 100 and 0 ka. Quat. Sci. Rev. 21, 1213–1228.

Hodell, D.A., Brenner, M., Curtis, J.H., Guilderson, T., 2001. Solar forcing of drought frequency in the Maya Lowlands. Science 292 (5520), 1367–1370. http://dx.doi.org/10.1126/science.1057759.

Haug, G.H., Hughen, K.A., Sigman, D.M., Peterson, L.C., Röhl, U., 2001. Southward migration of the intertropical convergence zone through the Holocene. Science 293 (5533), 1304–1308. http://dx.doi.org/10.1126/science.1059725.

Hoogakker, B.A.A., Chapman, M.R., McCave, I.N., Hillaire-Marcel, C., Ellison, C.R.W., Hall, I.R., Telford, R.J., 2011. Dynamics of North Atlantic Deep Water masses during the Holocene. Paleoceanography 26, PA4214. http://dx.doi.org/10.1029/2011PA002155.

Jaeschke, A., Rühlemann, C., Arz, H., Heil, G., Lohmann, G., 2007. Coupling of millennial-scale changes in sea surface temperature and precipitation off northeastern Brazil with high-latitude climate shifts during the last glacial period. Paleoceanography 22, PA4206. http://dx.doi.org/10.1029/2006PA001391.

Keigwin, L.D., Jones, G.A., 1994. Western North Atlantic evidence for the millennial-scale changes in circulation and climate. J. Geophys. Res. 99 (6), 397–412.

Kennett, J.P., Srinivasam, M.S., 1983. Neogene Planktonic Foraminifera: a Philogenetic Atlas. Hutchinson Ross Publishing Company, Stroudsburg 273.

Lamy, F., Hebbeln, D., Ro, U., Wefer, G., 2001. Holocene rainfall variability in southern Chile: a marine record of latitudinal shifts of the Southern Westerlies. Earth Planet. Sci. Lett. 185, 369–382.

Lorenz, S.J., Kim, J.-H., Rimbu, N., Schneider, R.R., Lohmann, G., 2006. Orbitally driven insolation forcing on Holocene climate trends: Evidence from alkenone data and climate modeling. Paleoceanography 21 (1), PA1002. http://dx.doi.org/10.1029/2005PA001152.

Marchal, O., Cacho, I., Stocker, T.F., Grimalt, J.O., Calvo, E., Martrat, B., Shackleton, N., Vautravers, M., Cortijo, E., van Kreveld, S., Anderson, C., Koç, N., Chapman, M., Sbaffi, L., Duplessy, J.-C., Sarnthein, M., Turon, J.-L., Duprat, J., Jansen, E., 2002. Apparent long-term cooling of the sea surface in the northeast Atlantic and Mediterranean during the Holocene. Quat. Sci. Rev. 21 (4–6), 455–483.

Mayewski, P., Rohling, E., Curtstager, J., Karlen, W., Maasch, K., Davidmeeker, L., Meyerson, E., Gasse, F., van Kreveld, S., Holmgren, K., Lee-Thorp, J., Rosqvist, G., Rack, F.,

Staubwasser, M., Schneider, R.R., Steig, R.J., 2004. Holocene climate variability. Quat. Res. 62 (3), 243–255. http://dx.doi.org/10.1016/j.yqres.2004.07.001.

Mayr, C., Wille, M., Haberzettl, T., Fey, M., Janssen, S., Lucke, A., Ohlendorf, C., Oliva, G., Schäbitz, F., Scheleser, G.H., Zolitschka, B., 2007. Holocene variability of the Southern Hemisphere westerlies in Argentinean Patagonia (52°S). Quat. Sci. Rev. 26 (5–6), 579–584. http://dx.doi.org/10.1016/j.quascirev.2006.11.013.

McDermott, F., Frisia, S., Huang, Y., Longinelli, A., Spiro, B., Heaton, T.H.E., Hawkesworth, C.J., Borsato, A., Keppens, E., Fairchild, I.J., van der Borg, K., Verheyden, S., Selmo, E., 1999. Holocene climate variability in Europe: evidence from d18O, textural and.extension-rate variations in three speleothems. Quat. Sci. Rev. 18, 1021–1038.

McManus, J.F., Francois, R., Gherardi, J.-M., Keigwin, L.D., Leger-Brown, S., 2004. Collapse and rapid resumption of Atlantic meridional circulation linked to deglacial climate changes. Nature 428, 834–837. http://dx.doi.org/10.1038/nature02494.

McDermott, F., Mattey, D.P., Hawkesworth, C., 2001. Centennial-scale Holocene climate variability revealed by a high-resolution Speleothem δ^{18}O record from SW Ireland. Science 294, 1328–1331.

Menary, M.B., Park, W., Lohmann, K., Vellinga, M., Palmer, M.D., Latif, M., Jungclaus, J.H., 2011. A multimodel comparison of centennial Atlantic meridional overturning circulation variability. Clim. Dyn. 38 (11–12), 2377–2388. http://dx.doi.org/10.1007/s00382-011-1172-4.

Morley, A., Schulz, M., Rosenthal, Y., Mulitza, S., Paul, A., Rühlemann, C., 2011. Solar modulation of North Atlantic central Water formation at multidecadal timescales during the late Holocene. Earth Planet. Sci. Lett. 308 (1–2), 161–171. http://dx.doi.org/10.1016/j.epsl.2011.05.043.

Moros, M., Emeis, K., Risebrobakken, B., Snowball, I., Kuijipers, A., McManus, J., Jansen, E., 2004. Sea surface temperatures and ice rafting in the Holocene North Atlantic: climate influences on northern Europe and Greenland. Quat. Sci. Rev. 23, 2113–2126. http://dx.doi.org/10.1016/j.quascirev.2004.08.003.

Niedermeyer, E.M., Schefuß, E., Sessions, A.L., Mulitza, S., Mollenhauer, G., Schulz, M., Wefer, G., 2010. Orbital- and millennial-scale changes in the hydrologic cycle and vegetation in the western African Sahel: Insights from individual plant wax delta D and δ^{13}C. Quat. Sci. Rev. 29 (23–24), 2996–3005. http://dx.doi.org/10.1016/j.quascirev.2010.06.039.

Nielsen, S.H.H., Koç, N., Crosta, X., 2004. Holocene climate in the Atlantic sector of the Southern Ocean: controlled by insolation or oceanic circulation? Geology 32 (4), 317. http://dx.doi.org/10.1130/G20334.1.

Olsen, J., Anderson, N.J., Knudsen, M.F., 2012. Variability of the North Atlantic Oscillation over the past 5,200 years. Nat. Geosci. 5, 808–812.

Parker, F.L., 1962. Planktonic foraminiferal species in Pacific sediments. Micropaleontology 8 (2), 219–254.

Pena, L.D., Francés, G., Diz, P., Esparza, M., Grimalt, J.O., Nombela, M.A., Alejo, I., 2010. Climate fluctuations during the Holocene in NW Iberia: high and low latitude linkages. Cont. Shelf Res. 30 (13), 1487–1496. http://dx.doi.org/10.1016/j.csr.2010.05.009.

Pokras, E.M., Mix, A.C., 1987. Earth's precession cycle and Quaternary climatic change in tropical Africa. Nature 326, 486–487.

Poore, R.Z., 2003. Millennial- to century-scale variability in Gulf of Mexico Holocene climate records. Paleoceanography 18 (2). http://dx.doi.org/10.1029/2002PA000868.

Risebrobakken, B., Jansen, E., Andersson, C., Mjelde, E., Hevrøy, K., 2003. A high-resolution study of Holocene paleoclimatic and paleoceanography changes in the Nordic Seas. Paleoceanography 18 (1). http://dx.doi.org/10.1029/2002PA000764.

Reimer, P.J., Baillie, M.G.L., Bard, E., Bayliss, A., Beck, J.W., Blackwell, P.G., Bronk Ramsey, C., Buck, C.E., Burr, G.S., Edwards, R.L., Friedrich, M., Grootes, P.M., Guilderson, T.P., Hajdas, I., Heaton, T.J., Hogg, A.G., Hughen, K.A., Kaiser, K.F., Kromer, B., McCormac, F.G., Manning, S.W., Reimer, R.W., Richards, D.A., Southon, J.R., Talamo, S., Turney, C.S.M., van der Plicht, J., Weyhenmeyer, C.E., 2009. IntCal09 and Marine09 radiocarbon age calibration curves, 0–50,000 years cal BP. Radiocarbon 51, 1111–1150.

Rohling, E.J., Pälike, H., 2005. Centennial-scale climate cooling with a sudden cold event around 8,200 years ago. Nature 434, 975–979. http://dx.doi.org/10.1038/nature03421.

Rousse, S., Kissel, C., Laj, C., Eiríksson, J., knudsen, K.-L, 2006. Holocene centennial to millennial-scale climatic variability: Evidence from high-resolution magnetic analyses of the last 10 cal kyr off North Iceland (core MD99-2275). Earth and Planetary Science Letters 242, 390–405. http://dx.doi.org/10.1016/j.epsl.2005.07.030.

Rühlemann, C., Mulitza, S., Lohmann, G., Paul, A., Prange, M., Wefer, G., 2004. Intermediate depth warming in the tropical Atlantic related to weakened thermohaline circulation: combining paleoclimate data and modeling results for the last deglaciation. Paleoceanography 19, PA1025. http://dx.doi.org/10.1029/2003PA000948.

Schulz, M., 2002. REDFIT: estimatingred-noise spectra directly from unevenly spaced paleoclimatic time series. Comput. Geosci. 28, 421–426.

Schulz, M., Stattegger, K., 1997. SPECTRUM: spectral analysis of unevenly spaced paleoclimatic time series. Comput. Geosci. 23 (9), 929–945.

Singh, A.D., Jung, S.J.A., Darling, K., Ganeshram, R., Ivanochko, T., Kroon, D., 2011. Productivity collapses in the Arabian Sea during glacial cold phases. Paleoceanography 26 (3), PA3210. http://dx.doi.org/10.1029/2009PA001923.

Skillbeck, C.G., Rolph, T.C., Hill, N., Woods, J., Wilkens, R.H., 2005. Holocene millennial/centennial-scale multiproxy cyclicity in temperate eastern Australian estuary sediments. JQS 20 (4), 327–347. http://dx.doi.org/10.1002/jqs.920.

Stramma, L., Fischer, J., Reppin, J., 1995. The north Brazil undercurrent. Deep-Sea Res. I Oceanogr. Res. Pap. 42 (5), 773–795.

Strikis, N.M., Cruz, F.W., Cheng, H., Karmann, I., Edwards, R.L., Vuille, M., Wang, X., de Paula, M.S., Novello, V.F., Auler, A.S., 2011. Abrupt variations in South American monsoon rainfall during the Holocene based on a speleothem record from central-eastern Brazil. Geology 39 (11), 1075–1078. http://dx.doi.org/10.1130/G32098.1.

Sutton, R.T., Jewson, S.P., Rowell, D.P., 2000. The elements of climate variability in the Tropical Atlantic Region. J. Clim. 13 (18), 3261–3284. http://dx.doi.org/10.1175/1520-0442.

Thompson, G.L., 2000. Ice core evidence for climate change in the Tropics: implications for our future. Quat. Sci. Rev. 19, 19–35.

Vinther, B.M., Buchardt, S.L., Clausen, H.B., Dahl-Jensen, D., Johnsen, S.J., Fisher, D.A., Koerner, R.M., Raynaud, D., Lipenkov, V., Andersen, K.K., Blunier, T., Rasmussen, S.O., Steffensen, J.P., Svensson, A.M., 2009. Holocene thinning of the Greenland ice sheet. Nature 461, 385–388. http://dx.doi.org/10.1038/nature08355.

Wang, Y., Cheng, H., Edwards, R.L., He, Y., Kong, X., An, Z., Wu, J., Kelly, M.J., Dykoski, C.A., Li, X., 2005. The Holocene Asian monsoon: links to solar changes and North Atlantic climate. Science 308 (5723), 854–857. http://dx.doi.org/10.1126/science.1106290.

Wanner, H., Beer, J., Bütikofer, J., Crowley, T.J., Cubasch, U., Flückiger, J., Goosse, H., Grosjean, M., Fourtunat, J., Kaplan, J.O., Küttel, M., Müller, S.A., Prentice, I.C., Solomina, O., Stocker, T.F., Tarasov, P., Wagner, M., Widmann, M., 2008. Mid- to Late Holocene climate change: an overview. Quat. Sci. Rev. 27 (19–20), 1791–1828. http://dx.doi.org/10.1016/j.quascirev.2008.06.013.

Wilson, K.E., Maslin, M.A., Burns, S.J., 2011. Evidence for a prolonged retroflection of the North Brazil Current during glacial stages. Palaeogeogr. Palaeoclimatol. Palaeoecol. 301 (1–4), 86–96. http://dx.doi.org/10.1016/j.palaeo.2011.01.003.

Wirtz, K.W., Lohmann, G., Bernhardt, K., Lemmen, C., 2010. Mid-Holocene regional reorganization of climate variability: analyses of proxy data in the frequency domain. Palaeogeogr. Palaeoclimatol. Palaeoecol. 298 (3–4), 189–200. http://dx.doi.org/10.1016/j.palaeo.2010.09.019.

Yu, Y., Yang, T., Li, J., Liu, J., An, C., Liu, X., Fan, Z., Lu, Z., Li, Y., Su, X., 2006. Millennial-scale Holocene climate variability in the NW China drylands and links to the tropical Pacific and the North Atlantic. Palaeogeogr. Palaeoclimatol. Palaeoecol. 233 (1–2), 149–162. http://dx.doi.org/10.1016/j.palaeo.2005.09.008.